

FIBER DAMAGE IMPARTED BY 3D ORTHOGONAL WEAVING OF PITCH CARBON AND CERAMIC YARNS

K.W. Sharp and A.E. Bogdanovich
3TEX
109 MacKenan Dr.
Cary, NC USA
sharpk@3TEX.com

SUMMARY

Bending and abrasion of high modulus fibers during weaving can cause yarn failure. In non-crimp 3D orthogonal weaving, the primary limitation is the bend radius of the Z yarns at the fabric surface. Trials with ceramic and pitch carbon yarns have related the 3D orthogonal weaving limitations to a model of the internal stresses of a single fiber.

Keywords: 3-D weaving, ceramic fibers, pitch carbon fibers, CMC, oxide-oxide composites

INTRODUCTION

Compared to traditional uniaxial or biaxial laminates, 3D woven fiber architectures have been shown to increase interlaminar strength, impact resistance, and damage tolerance of polymer matrix [1] and ceramic matrix composites (CMC's) [2,3]. 3D weaving processes have also enabled the production of preforms that match a wide variety of complex near net shapes. These attributes have led to the use of composites based on 3D woven preforms in commercial applications as diverse as boat hulls, structural I-beams in buildings, manhole covers, and components in aircraft [4].

3D fiber architectures also provide the opportunity for enhanced through thickness thermal and electrical properties in composites. As an example, placing pitch carbon yarns in the through thickness (Z) positions of a non-crimp 3D orthogonal weave enabled the production of composites that increased the through thickness thermal conductivity 12 fold over that of traditional laminated composites [5].

Most of the reported research on 3D fiber architectures has involved composites based on preforms fabricated by a warp interlock 3D weaving process. This process utilizes 2D weaving machines adapted with cam, dobby, or Jacquard shedding mechanisms to arrange the warp yarns throughout the multiple layers of the fabric preform [6]. For composites based on the warp interlock 3D preforms, the interlaminar property improvements are offset by reductions in the in-plane mechanical properties [7,8]. Although the primary cause for the loss of tensile and compressive strength in this form of 3D woven composites was due to the waviness or crimp of the warp yarns in the fiber architecture [8], the multiple manipulations of the warp yarns required in the interlock weaving process were also shown to impart significant fiber damage in the warp yarns [6,9].

Both the ceramic yarns used in the CMC's and the pitch carbon yarns used to improve the thermal conductivity of the polymer composites are composed of brittle fibers that are difficult to weave and are susceptible to damage due to abrasion and flexure during processing. A less widely studied 3-D fiber architecture, which we will call non-crimp 3D orthogonal following [6], is manufactured using that provides an advantage over warp interlock 3-D weaving by the reducing the amount of manipulation, thus reducing abrasion and flexure, of the yarns during fabric processing. Further, as a result of the uncrimped, straight warp and fill yarns, polymer matrix composites based on this form of 3-D fiber architecture have shown improved interlaminar properties without a loss of in-plane stiffness or strength [8,10]. The research presented here involves several experiments involving the manufacture of preforms on non-crimp 3D orthogonal weaving machines.

FIBER DAMAGE IN WEAVING

Two dominant sources of damage to or failure of high modulus, brittle fibers during processing are the generation of high internal stresses in the fibers by the bending imposed during the weaving process and the abrasion of the yarns on contact surfaces of the weaving machines.

Critical Fiber Radius

Although a yarn is composed of hundreds or thousands of individual fibers that bend to a number of radii as the yarn is formed to a given shape, determination of the limiting bend radius of a single pristine fiber can provide a lower bound for the radius to which a yarn bundle may be formed. As described in [11], the internal tensile/compressive stresses generated in a single fiber bent to a given radius can be estimated by Equations (1) and (2) [12], where ε is strain, s is the arc length of the outside of the fiber, s_0 is the arc length of the center of the bent fiber, r is the fiber radius, and R is the bend radius. For a brittle fiber, the critical radius, R_c , below which the single fiber will fracture can be calculated, given the fiber modulus E and the fiber ultimate tensile strength σ_c .

$$\varepsilon = \frac{s - s_0}{s} = \frac{r}{R + r} \quad (1)$$

$$R_c = \frac{r}{2} \left[\frac{E}{\sigma_c} - 1 \right] \quad (2)$$

Other factors not considered in this simple model also influence the ability to weave a yarn, including sizing, anisotropy in the fiber's mechanical properties, variation in the strength of individual fibers in a yarn, the ability of the fibers to withstand abrasion, the surface damage accumulated during processing, the yarn's friction, and the yarn's tendency to fray. Each of these factors further limits the formation of fabrics made from the high modulus fibers. Thus the R_c calculated in Equation (2) can be considered the minimum bending radius to which a yarn of brittle fibers can be formed, providing a general guide for the limits of the final fiber architecture and for the radii of weaving machine components. The R_c value also allows a first order comparison of the potential difficulty of weaving yarns of various fibers.

Abrasion

During weaving, individual yarns contact a number of guides and tension devices and cross or rub other yarns as they are formed into a fabric. In 2-D weaving, guides (which are called heddles) reposition all warp yarns after each weft yarn insertion across the fabric, subjecting the yarns to a substantial degree of abrasion as the yarns pass over the radii of the heddles at high tension. The weft yarns are inserted with much less abrasion either with rapiers or air jets.

Warp interlock 3D weaving also repositions heddles containing all or most of the warp yarns at each weft insertion, with a separate weft insertion for the formation of each fabric layer [13]. The numerous heddle motions required for multiple layer fabrics can cause significant fiber damage to each warp yarn. One study found a 50% reduction of the warp yarn strength in E-glass warp interlock 3-D weaving [9].

NON-CRIMP 3-D ORTHOGONAL WEAVING

Non-Crimp Orthogonal 3-D Weave Architecture

In non-crimp orthogonal 3-D weaving, such as the multi-rapier process invented in [14] and further developed by 3TEX [10], all filling layer yarns are simultaneously inserted in a single machine cycle and only the through thickness (Z) yarns are repositioned by heddles. The fiber architecture contains a number of warp layers and one more fill than warp layers, so that the fill layers occupy the outermost positions in the fabric. The Z yarns then bind the fabric by crossing over/under the outermost fill layers. Figure 1 shows the resultant fiber architecture.

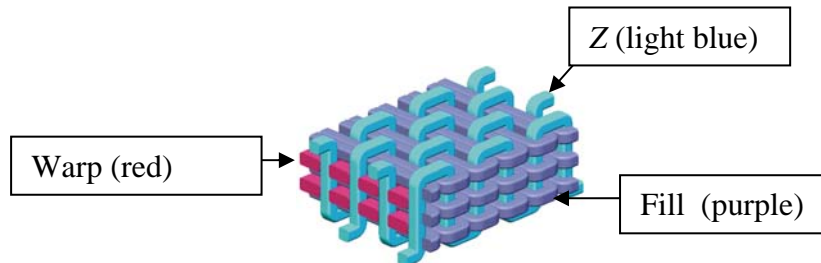


Figure 1. Non-crimp 3D Orthogonal Weave Fiber Architecture.

Non-crimp 3-D Orthogonal Weaving Process

In the non-crimped 3-D orthogonal weaving process performed on a multi-rapier 3-D weaving machine, the warp yarns are aligned along the length of the fabric and are directed from a creel where the yarn bobbins are held, through a comb-like structure called a reed. The reed positions the warp yarns directly into the fabric without further manipulation, remaining uncrimped in the resultant fabric. The Z yarns enter the reed alongside the warp yarns, but prior to entering the reed, they are threaded through heddles. The heddles are equally divided between top and bottom harnesses that move in opposite vertical directions after the fill yarn insertion. For a more complete description of the multi-rapier 3-D orthogonal weaving process see [6,14].

In this non-crimped 3-D orthogonal weaving process, the warp yarns do not undergo any significant bending, while the fill yarns are subjected to bending primarily at the

selvedge loops. The Z yarns, in contrast, wrap around the top or bottom fill yarns to form a relatively small radius, which is the critical radius in this fiber architecture. The ability of Z yarns to withstand this bending restricts the fill yarn spacing per unit length. This maximum fill yarn spacing, FS_{max} is the inverse of the minimum bend diameter. This relation is described in Equation (3).

$$FS_{max} = \frac{1}{2R_c} \quad (3)$$

3-D ORTHOGONAL WEAVING OF CERAMIC FIBERS

CMC's fabricated from textile preforms have long been investigated for their ability to withstand high temperatures while providing much higher damage tolerance than monolithic ceramics. CMC's have demonstrated sufficient strength and stiffness to carry some structural load [15,16]; improved fracture toughness, especially those based on 3-D architectures [17,18]; and the ability to withstand hours of exposure to high temperature [19]. Applications for CMC's include components in gas turbine engines for aircraft and for electrical power generation, as well as thermal protection systems for spacecraft and re-entry vehicles. A wide variety of ceramic fibers, ceramic matrices, and fiber architectures, each corresponding to various operating regimes and temperatures, have been reported in the literature and many are in commercial use.

Ceramic Fiber Properties

Ceramic fibers have high modulus and fail in a brittle fashion. Table 1 lists some mechanical properties of commercial ceramic fibers, sorted in order of the calculated R_c value. Manufacturer's data was used as the source for the fiber properties, unless otherwise referenced. The final column contains the maximum fill yarn spacing, FS_{max} , determined from R_c .

Table 1. Commercially Available Ceramic Fibers with their R_c and FS_{max} values.

Fiber type	Fiber Material	Fiber Dia. (μm)	Tensile Modulus (GPa)	UTS (MPa)	R_c (mm)	FS_{max} (/cm)
Tyranno LOX M [20]	SiC	8.5	180	2500	0.30	16.7
Tyranno ZMI [20]	SiC	11	200	3400	0.32	15.6
Nextel 440	AlO ₂ -SiO ₂	11	190	2000	0.52	9.6
Nextel 550	AlO ₂ -SiO ₂	11	193	2000	0.53	9.4
Sylramic	SiC	10	400	3200	0.62	8.1
Nicalon NL200	SiC	14	190	2000	0.66	7.6
Hi-Nicalon	SiC	14	263	2600	0.70	7.1
Tyranno SA [21]	SiC	10	420	2800	0.74	6.8
Nextel 610	Al ₂ O ₃	11	380	3100	0.67	6.5
Nextel 720	Al ₂ O ₃	11	260	2100	0.67	6.5
Hi-Nicalon S	SiC	12	410	2600	0.94	5.3
Saphikon [20]	Al ₂ O ₃	125	471	3500	8.34	0.6

From the R_c calculations listed, the alumina Nextel 610 and alumina-mullite Nextel 720 yarns should be among the most difficult commercial ceramic yarns to weave. When formed as Z yarns in a non-crimp 3-D orthogonal fabric, the maximum fill yarn spacing should be less than 6.5 fill insertions per cm.

3-D Weaving Experiments

Weaving trials of Nextel 610 and 720 yarns were conducted on multi-rapier, non-crimp 3D orthogonal weaving machines at 3TEX. In one trial, a 6 warp layer fiber architecture with Nextel 720 in all yarn positions successfully produced a fabric at a maximum fill yarn spacing of 4.9 /cm [22]. In another trial, a hybrid 3-D orthogonal fabric comprised of Nextel 610 in the warp and fill yarns, with Nextel 610 in five of the Z yarn positions and Nextel 720 in the remainder of the Z yarn positions achieved a fill yarn spacing of 4.3 /cm without reaching failure in the yarns [11]. Figure 2 shows images of each fabric.

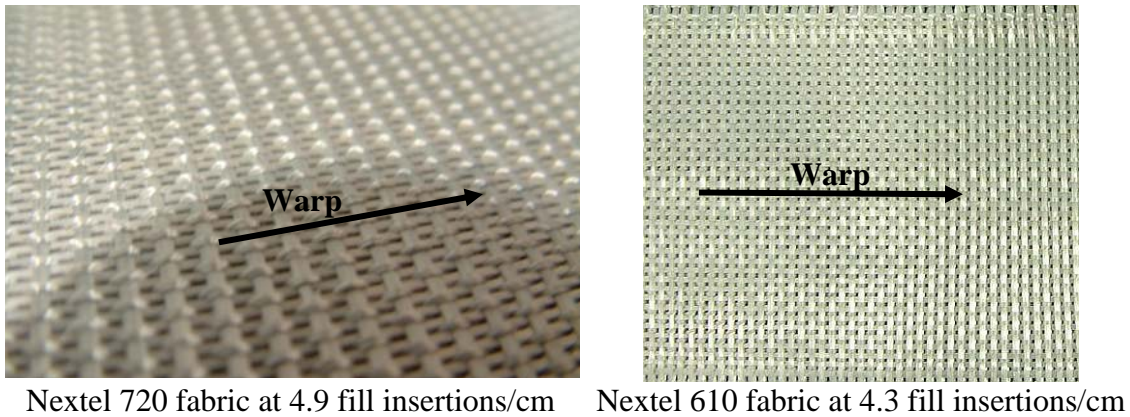


Figure 2. 3-D Orthogonal Nextel 610 fabric

The maximum fill yarn spacing achieved in the tests on the Nextel 610 and 720 yarns were between $2/3$ and $3/4$ of the calculated FS_{max} . Correspondingly, the critical radius for the yarn within the fiber architecture for these fabrics would be 1.2 mm for the Nextel 610 and 1.0 mm Nextel 720, approximately 1.5 to 1.8 times the single pristine fiber R_c calculated for the fibers. As described above, this increase in R_c is due to a combination of abrasion, sizing, and individual fiber variations within the yarn bundles.

The implication of these results is that as a first order approximation, the bend radii in fiber architectures with ceramic fibers will likely be limited to between $1 \frac{1}{2}$ to 2 times the pristine fiber R_c . Further, weaving machine components intended for use with ceramic fibers should be designed with radii greater than 2 times the R_c value.

Since the Z yarn experiences the smallest bend radius, the fact that even the Nextel 720 yarns could be used in Z yarn position of the non-crimp 3-D orthogonal fiber architecture implies that almost all the ceramic fibers listed in Table 1 can be non-crimp 3-D orthogonally woven in all yarn positions. Only Saphikon is unlikely to be successfully woven in the Z direction of an orthogonal 3-D weave, although there is a high likelihood that it can be woven in the fill or warp yarn positions.

3-D ORTHOGONAL WEAVING OF PITCH CARBON FIBERS

Pitch carbon fibers are composed of significant fractions of aligned graphite layers, with tensile modulus, tensile strength, and axial electrical and thermal conductivity increasing as the graphite content increases. The most highly graphitized pitch carbon fibers can have thermal conductivity as high as 950 W/mK, well in excess of pure copper at 400 W/mK. In some applications, e.g. electrical buses in spacecraft or enclosures around high heat sources such as gearboxes, the reduction in weight provided by composites is offset by their lower thermal conductivity compared to metals. The use of pitch carbon fibers within a composite can increase the composite's thermal conductivity in some directions beyond that of the metals and enable its use in these types of applications.

Since graphite exhibits a high level of anisotropy, as the fibers become more graphitic and the axial modulus and thermal conductivity increases, their transverse shear strength decreases. So, in addition to brittle failure in bending, the yarns can fail in transverse shear mode as loads are applied radially to the fiber. Such loads may be imposed by the motion of the heddles after the fill yarn insertion and by lateral compression of the yarns during the beat-up phase after the fill insertion.

Pitch Carbon Fiber Properties

Table 2 lists some mechanical properties of commercial pitch carbon fibers, as well as calculations of R_c and the maximum fill yarn spacing, FS_{max} . Manufacturer's data provides the references for the fiber properties. The R_c are generally larger than those for the ceramic fibers, with the FS_{max} values correspondingly larger. This shows that, even without regard to the loss in shear strength, the pitch carbon yarns should be more difficult to weave than the ceramic yarns.

Table 2. Commercially Available Pitch Carbon Fibers with their R_c and FS_{max} values.

	Axial Thermal Conductivity (W/mK)	Fiber Dia. (μm)	Tensile Modulus (GPa)	Tensile Strength (MPa)	R_c (mm)	FS_{max} (/cm)
Hexcel IM7 (PAN)	8	5	275	5300	0.13	38.5
Toray T300 (PAN)	10	7	230	3700	0.21	23.8
Granoc YS80	320	7	785	3630	0.75	6.6
Granoc CN60	180	10	600	3500	0.85	5.9
Granoc YS90	500	7	880	3530	0.87	5.7
Granoc YS95	600	7	900	3530	0.89	5.6
Granoc CN80	320	10	780	3430	1.13	4.4
Mitsubishi K13C2U	620	10	900	3800	1.18	4.2
Mitsubishi K13D2U	800	11	935	3700	1.38	3.6
Cytec K1100	950	10	965	3100	1.55	3.2
Thornel P-120S	370	10	827	2410	1.71	2.9

Pitch Carbon 3-D Weaving Experiments

A series of weaving trials have been conducted to determine the ability to manufacture non-crimp 3-D orthogonal woven fabrics with the pitch carbon yarns in the Z yarn position. Those trials were performed on one of the multi-rapier 3D weaving machines at 3TEX [11]. In the trials, the fill yarn spacing was decreased until the Z yarns began to fracture at the bend radius at the surface of the preform. Once the limiting fill spacing with the pitch carbon in the Z yarn position was established, the pitch carbon yarn was placed in a fill yarn position in the fiber architecture and its ability to be woven in that position was tested. A final weaving test in the warp yarn position was only conducted on those yarns that failed in the fill yarn weaving test.

Table 3 shows the results of tests with a number of different pitch carbon fibers. For each fiber type, the maximum fill yarn spacing achieved with the fiber in the Z direction is listed. If the yarn was not weavable in the Z direction, the results of the tests whether the yarn could be woven in the fill and warp directions are listed.

Table 3. Weaving Test Results for Pitch Carbon Yarns.

	Axial Thermal Conductivity (W/mK)	R_c (mm)	FS_{max} (/cm)	Test Fill Yarn spacing at Yarn Failure (/cm)
Granoc YS80	320	0.75	6.6	2.6
Granoc CN60	180	0.85	5.9	2.2
Granoc YS90	500	0.87	5.7	Fill and Warp only
Granoc YS95	600	0.89	5.6	2.2
Granoc CN80	320	1.13	4.4	2.1
Mitsubishi K13C2U	620	1.18	4.2	Fill and Warp only
Mitsubishi K13D2U	800	1.38	3.6	Not weavable in standard form
Cytec K1100	950	1.55	3.2	Not weavable in standard form

The maximum fill yarn spacing achieved in the tests with the Granoc pitch carbon yarns was between 2/5 and 1/2 of the calculated FS_{max} , a much lower fraction than for the Nextel ceramic yarns. This corresponds to a minimum bend radius that was 2.1 to 2.8 times greater than the estimated R_c , a higher ratio than was found for the ceramic fibers. The ratio of the demonstrated bend radius in the tested fiber architecture to the estimated R_c of the single pristine pitch carbon fiber was increased compared to the case of the ceramic yarns. This is most likely due to the lower shear strength of the pitch carbon fibers.

The implication of these results is that, as a first order approximation, bend radii in fiber architectures with pitch carbon fibers will likely be limited to between 2 to 3 times the pristine fiber R_c . Further, weaving machine components intended for use with pitch carbon fibers should be designed with radii more than 3 times the R_c value. Also, machine operations should avoid the application of shear loads as much as is possible.

The Cytex K1100 and the Mitsubishi K13D2U, in their standard sizing, could not be woven in a 3-D orthogonal architecture, failing as the reed advanced to consolidate the fabric after a fill yarn insertion (“beat up”), even when used in the warp yarn position. The addition of a thicker sizing layer on the yarns may increase the shear strength sufficiently for it to survive the beat up process without damage. Another method that could be used to provide increased shear strength is to “serve” the yarns, i.e. wrap the yarns with a small fiber having higher shear strength.

3D Weaving Pattern Modifications to Increase the Fill Yarn Spacing

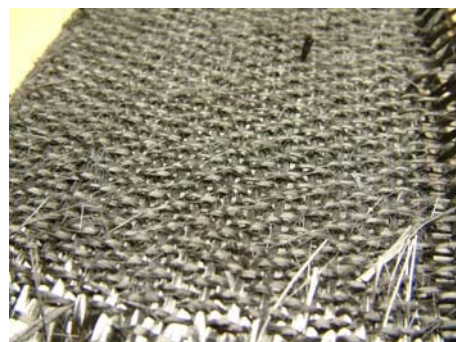
A second set of tests was conducted on the YS80 and CN80 yarns. An additional set of harnesses and heddles were added to the weaving machine to place two Z yarns along each warp yarn position rather than the single Z yarn per warp yarn position as in the previous set of tests. The weaving pattern was then modified so that any individual Z yarn would only be inserted through the fabric after two fill insertions, yet sequenced so that one of the Z yarns would be inserted through the fabric after each fill insertion. Since individual Z yarns only exchange positions on alternate fill insertions, they were subjected to a bend radius approximately twice that of the first 3-D orthogonal weave pattern. The use of an additional set of Z yarns in the warp yarn positions maintained a high fiber volume of Z yarns through the thickness of the fabric. In these tests, the fill yarn spacing improved as follows,

- YS 80 increased from 2.6/cm in the first pattern to 4.5/cm in the modified pattern.
- CN80 increased from 2.1/cm in the first pattern to 3.0/cm in the modified pattern.

For the through thickness thermal conductivity tests described in [5], 13 mm thick preforms were manufactured with YS 80 in the Z yarn positions using this modified weaving pattern. The thicker preform increased the amount of shearing and abrasion imposed upon the Z yarns as they passed through the warp yarns during the weaving cycle, in turn reducing the maximum fill yarn spacing that could be attained. Figure 3 shows the upper surfaces of two such 13 mm thick preforms, one woven at 2.4 fill yarn insertions/cm and the other at 3.1. The increase in damage that can be seen in the Z yarns at the bend radii as the fill spacing increased was typical of all of the fabrics with pitch Z yarns.



a) 2.4 Fill Insertions/cm



b) 3.1 Fill Insertions/cm

Figure 3. Comparison of 13 mm Thick Preforms with Modified 3-D Orthogonal Weave Patterns at Two Fill Yarn Spacings

CONCLUSIONS

High modulus, brittle fibers, such as ceramic and pitch carbon, pose special problems to 3-D weaving due to the internal stresses generated by the bending of the fibers and to abrasion that occur during processing. Non-crimp 3-D orthogonal weaving minimizes the manipulation of the yarns and this provides an advantage in the fabrication of high modulus fiber preforms over warp interlock 3-D weaving. In non-crimp 3-D orthogonal fiber architecture, the through thickness (*Z*) yarn is subjected to the most critical stresses during weaving, while the warp yarns are subjected to only minimal stresses.

A model of the internal stresses generated in a single, pristine fiber was found to describe a lower bound for the radius to which a yarn bundle of high modulus, brittle fibers can be formed, as well as providing a general guideline for the relative difficulty of weaving a particular fiber type. This critical radius was correlated to a maximum fill yarn spacing.

3-D weaving experiments showed that Nextel 610 and Nextel 720 ceramic yarns, two of the more difficult ceramic fibers to weave, could be woven in the *Z* yarn positions at approximately 1.5 to 1.8 times the lower bound radius determined by the model. This leads to the general guideline that, when weaving ceramic fibers, weaving machine components should have radii greater than 2 times the critical radius of the pristine fiber and the fiber architectures in non-crimp 3D orthogonal weaving should not form the yarns to below 1 ½ to 2 times the critical radius.

The high level of anisotropy and low shear strength of pitch carbon yarns compound the difficulty of weaving them. A series of weaving experiments on a variety of pitch carbon yarns had determined which yarns could be 3-D orthogonally woven in their “as delivered” state. These tests demonstrated weaving in the *Z* yarn positions at 2.1 to 2.8 times the lower bound radius for several pitch carbon yarns, though some of the most highly graphitic yarns could not be woven even in the warp position.

The general guidelines developed from the testing of pitch carbon yarns are more stringent than those for 3D weaving ceramic yarns. Weaving machine components should have radii greater than 3 times the critical radius of the pristine fiber and should minimize the application of transverse shear loads applied to the yarns. The yarns in a non-crimp 3D orthogonal weaving fiber architectures should not be bent to a radius below 2 to 3 times the pitch carbon fiber’s critical radius.

References

1. V. Tamuzs, S. Tarasovs, and U. Vilks, *Composites Science and Technology*, **63**, 2003, pp 1423-1431.
2. D.C. Phillips, *J. Mat. Sci.*, **9**, pp. 1847-1854, (1974).
3. A.G. Evans and F.W. Zok, *J. Mat. Sci.*, **29**, pp. 3857-3896, (1994).
4. A.P. Mouritz, M.K. Bannister, P.J. Falzon, and K.H. Leong, *Composites Part A*, **30**, pp. 1445-1461, (1999).

5. K. Sharp, A.E. Bogdanovich, W. Tang, D. Heider, S. Advani, and M. Glowania,, AIAA Journal, Vol. 46 No. 11, pp. 2944-2973, Nov. 2008.
6. M. Mohamed, A.E. Bogdanovich, "Comparative Analysis of Different 3D Weaving, Processes, Machines, and Products, Proceedings of the 17TH International Conference On Composite Materials (ICCM-17), 27-31 July 2009, Edinburgh, UK.
7. T.R. Guess and E.D. Reedy, Journal of Composites Technology & Research, **7** (4), pp. 136-142, (1985).
8. J. Brandt, K. Dreschsler, and F-J. Arendts, Composites Science and Technology, **56**, pp. 381-386, (1996).
9. S. Rudov-Clark, A.P. Mouritz, L. Lee, and M.K. Bannister, Composites Part A, **34** , pp. 963-970 (2003).
10. M.H. Mohamed, A.E. Bogdanovich, L.C. Dickinson, J.N. Singletary, and R.B. Lienhart, SAMPE Journal, **37**, (3), 8-17, (2001).
11. K. Sharp and A. E. Bogdanovich, "3-D Weaving of Exotic Fibers: Lessons Learned and Success Achieved", Proceedings of SAMPE 2008, Long Beach, CA, May 18-22, 2008.
12. F. Ko, Ceramic Bulletin (ACers), **68** (2), 402 (1989).
13. Tong, A.P. Mouritz, and M.K. Bannister, 3D Fibre Reinforced Composite Materials, London: Elsevier, 2002.
14. M.H. Mohamed and Z. Zhang, U.S. Patent 5,085,252 (1992).
15. Yun, H.M, DiCarlo, J.A., and Fox, D.S., NASA TM-2004-213335, Sep 2004.
16. Evans, A.G., High Temperature Structural Materials, edited by R.W. Cahn et al, Chapman and Hall, London, 1996, pp. 94-108.
17. G. Ojard, T. Araki, S. Nishide, K. Watabe, F. Linsey and J. Anderson, Ceramic Engineering and Science Proceedings, **23**, [3], pp. 599-606 (2002).
18. Ogasawara, T. Ishikawa, H .Ito, N. Watanbe, and I. J. Davies, Journal of American Ceramic Society, **84**, [7], pp. 1565-74, (2001)
19. DiCarlo, J.A. et al., NASA TM-2004-213048, Nov. 2004.
20. A. Bunsell and M. Berger, Fine Ceramic Fibers, Marcel Dekker, New York - Basel, 1999. p 39.
21. T. Hinoki, L.L. Snead, E. Lara-Curzio, Y. Katoh, and A. Kohyama, Fusion Materials Volume 29 Semiannual Progress Report, DOE/ER313/29.
22. K.W. Sharp, A.E. Bogdanovich, D. Mungalov, D. Wigent, M.M. Mohamed, Proceedings of the SAMPE Fall Technical Conference 2005, Seattle, Nov 2005.